

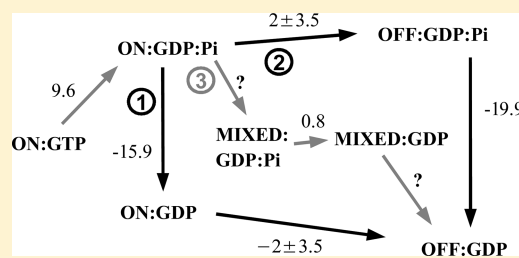
Conformational Selection by the aIF2 GTPase: A Molecular Dynamics Study of Functional Pathways

Priyadarshi Satpati and Thomas Simonson*

Laboratoire de Biochimie (CNRS UMR7654), Department of Biology, Ecole Polytechnique, 91128 Palaiseau, France

Supporting Information

ABSTRACT: Archaeal initiation factor 2 (aIF2) is a GTPase involved in protein biosynthesis. In its GTP-bound, “ON” conformation, it binds an initiator tRNA and carries it to the ribosome. In its GDP-bound, “OFF” conformation, it dissociates from tRNA. To improve our understanding of the role of each conformational state in the aIF2 “life cycle”, we start from the state immediately after GTP hydrolysis, ON:GDP:P_i (where P_i is inorganic phosphate), and consider the possible next steps on the pathway to the OFF:GDP product. The first possibility is P_i dissociation, leading to ON:GDP, which could then relax into OFF:GDP. We use molecular dynamics simulations to compute the P_i dissociation free energy and show that dissociation is highly favorable. The second possibility is conformational relaxation into the OFF state before P_i dissociation, to form OFF:GDP:P_i. We estimate the corresponding free energy approximately, 2 ± 3.5 kcal/mol, so that this is an uphill or weakly downhill process. A third possibility is relaxation into another conformation, neither ON nor OFF. Indeed, a third, “MIXED” conformation was seen recently in a crystal structure of the aIF2:GDP:P_i complex. For this conformational state, P_i dissociation is weakly unfavorable, in contrast to the ON and OFF states. From this, we will deduce that if the MIXED:GDP complex is not too unstable, the ON:GDP:P_i → MIXED:GDP:P_i transformation is a downhill process, which can occur spontaneously. This suggests that the MIXED state could be a functional intermediate.



Archaeal initiation factor 2 (aIF2) participates in the translation of mRNA into protein. It belongs to the GTPase family of proteins, which undergo conformational switching under the control of GTP or GDP binding^{1–5} and frequently serve as molecular switches for the timing and activation of biological events. Thus, aIF2 cycles between two distinct conformations, which have different nucleotide binding preferences and different functional roles. The active or “ON” conformation is stabilized by GTP binding; it is competent to bind an initiator tRNA and form an initiator complex with the ribosome. The inactive or “OFF” conformation is stabilized by GDP binding; this conformation dissociates from tRNA and the ribosome. Crystal structures have been reported for aIF2 in its ON and OFF conformations.^{6–8} The protein is composed of three subunits: α , β , and γ ; the main differences between the ON and OFF conformations are localized in two regions of the γ subunit, called switch 1 and switch 2, which are close to the nucleotide binding site and contain 20 amino acids each.

In two previous articles, we used molecular dynamics simulations to study the GTP/GDP binding specificities of the ON and OFF states of aIF2.^{9,10} Here, we focus on a different complex, the posthydrolysis complex of aIF2, GDP, and P_i (inorganic phosphate). Because aIF2:GTP is predominantly in the ON conformation, the state reached immediately after hydrolysis is most likely ON:GDP:P_i (where ON represents aIF2 in its ON conformational state). This complex can then either dissociate, giving ON:GDP and P_i, or relax into the OFF conformation, giving OFF:GDP:P_i. A third possibility is to relax into another conformational state. Indeed, a crystal structure of

the *Sulfolobus solfataricus* protein showed that aIF2:GDP:P_i can occupy a third, distinct conformation, here termed the “MIXED” state.⁷ In this state, switch 2 is in its ON conformation while switch 1 occupies a new conformation, neither ON nor OFF. With its ON switch 2 arrangement, the MIXED structure may be competent to bind tRNA. It is not clear whether the MIXED conformation is specifically stabilized by the presence of GDP and P_i or whether it is mainly stabilized by the crystal environment and/or buffer conditions. Indeed, in the ON and OFF states, the bound nucleotide (GTP or GDP) has an associated Mg²⁺ ion, which interacts directly with switch 1 in the ON state and with switch 2 in the ON and OFF states. In contrast, the MIXED state could only be crystallized under conditions where free Mg²⁺ is rare, and there is no Mg²⁺ ion visible in the MIXED:GDP:P_i crystal structure. The authors have suggested that the posthydrolysis complex, aIF2:GDP:P_i, is an important functional state, intermediate between the ON and OFF states, with a stability and lifetime that allow it to be observed crystallographically.⁷ A similar proposal has been made for other GTPases, including Ras and EF-Tu.^{11,12} For eIF2, the eukaryotic orthologue of aIF2, it was also suggested that the release of P_i from the protein is a distinct and important functional step, triggered by start-site selection on the mRNA.¹³

Received: November 6, 2011

Revised: December 9, 2011

Published: December 14, 2011



To examine the steps that follow GTP hydrolysis, we use molecular dynamics (MD) simulations. MD can be a valuable tool for studying protein–ligand recognition and conformational stability. In particular, molecular dynamics free energy simulations, or MDfE, can provide binding free energy differences and establish a direct link between microscopic structures and free energies.^{9,14–16} MDfE has been used to study nucleotide binding by several GTPases and ATPases.^{9,10,17–21} Here, we simulate dissociation of P_i from the $\alpha F2$:GDP complex in its ON, OFF, and MIXED states. An “alchemical” method is used,^{22–24} in which P_i is gradually deleted from the protein and reintroduced into the solution over a series of MD simulations. The protein and surrounding solvent are treated in atomic detail. The results allow us to determine the free energy for dissociation of P_i from each complex. We also consider the possibility of conformational relaxation into the OFF state before P_i dissociates. Using the previously published data,¹⁰ we quantify (albeit less precisely) the corresponding $ON:GDP:P_i \rightarrow OFF:GDP:P_i$ free energy change. Finally, we consider the $ON:GDP:P_i \rightarrow MIXED:GDP:P_i$ transformation. Characterizing its free energy is more difficult, for reasons discussed below. Here, we obtain only weak, indirect evidence, suggesting this free energy is indeed negative, so that spontaneous relaxation may occur.

To obtain reliable free energy results, we must address several difficulties, which were discussed in a recent paper.⁹ One is to construct structural models of the weakly populated, minor states, for which crystal structures are not available: $ON:GDP$, $ON:GDP:P_i$, $OFF:GDP:P_i$, and $MIXED:GDP$. Another is to determine the protonation state of several groups in the nucleotide binding pocket, including the GDP and P_i ligands themselves. This is done through specific free energy simulations. A third difficulty is to achieve sufficient conformational sampling, through long MD simulations, totalling more than 300 ns. Finally, a Mg^{2+} ion coordinates the GDP and P_i in the ON and OFF complexes but not the MIXED complex; therefore, comparison to the MIXED state will be sensitive to the details of the Mg^{2+} description. The system is modeled by a molecular mechanics force field, whose accuracy is necessarily imperfect.^{25,26} To reduce the sensitivity to force field details, we will compare the ON and OFF complexes and the MIXED complex to two different reference systems: P_i and Mg^{2+} in solution and P_i alone in solution, respectively.

This paper is organized as follows. In Materials and Methods, we introduce two thermodynamic cycles to compare P_i deletion in the protein and in solution, one for the ON and OFF states and one for the MIXED state. We describe the structural models used, the MD simulation setup, and the detailed protocol used for alchemical P_i deletion. In the Supporting Information, we describe free energy calculations used to determine the protonation of GDP, P_i , and a protein side chain in the MIXED state, and we provide details about the uncertainty of the MD free energy simulations. In Results, we first characterize dissociation of P_i from the ON and OFF complexes and from the MIXED complex. Next, we estimate the free energy for $ON:GDP:P_i$ to relax into $OFF:GDP:P_i$, and we analyze the effect of the phosphate on the relative stabilities of the ON and MIXED states. The last section summarizes our conclusions.

MATERIALS AND METHODS

Thermodynamic Cycle for Studying P_i Binding. To calculate the standard free energy of binding of P_i to the individual protein states, we use an alchemical method^{22–24} and

follow the horizontal legs of the thermodynamic cycles in Figure 1. Cycle 1 is used for both the ON and OFF states;

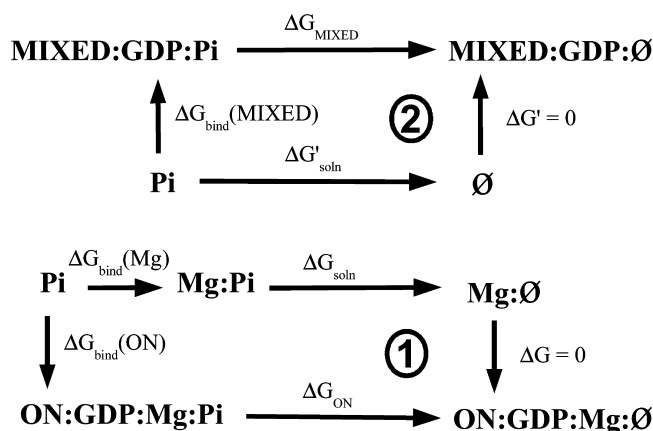


Figure 1. Thermodynamic cycles for binding of P_i to the MIXED state (cycle 1) and the ON or OFF state (cycle 2). Horizontal legs correspond to the alchemical transformation of P_i into a ghost particle (\emptyset) in the solvated protein (top and bottom) or in water (middle).

cycle 2 is used for the MIXED state. Each horizontal leg transforms the P_i group into a “ghost” particle (denoted “ \emptyset ”), either in complex with the protein (top, bottom legs) or in solution (middle legs). The ghost particle is a P_i that is “decoupled” from its environment and has effectively been removed to the gas phase. The transformation free energies (ΔG_{ON} or ΔG_{OFF} , ΔG_{soln} , ΔG_{MIXED} , and $\Delta G'_{soln}$) are computed using MD free energy simulations, or MDfE (see below). The solution leg is done differently in the two cycles. In cycle 2, we transform P_i into a ghost particle, effectively removing it to the gas phase. In cycle 1, we first bind P_i to a Mg^{2+} ion and then transform it. By using two distinct cycles, we expect that error compensation between the protein and solution simulations will be optimal. Indeed, an associated Mg^{2+} is present in the ON and OFF states, but absent from the MIXED state. The free energy $\Delta G_{bind}(Mg)$ for the first step in the cycle 1 solution leg is the $Mg^{2+}:P_i$ binding free energy, which will be taken from experiment.²⁷ By using cycle 1 for the ON and OFF states, we ensure that $Mg^{2+}-P_i$ interactions are present in both the protein and solution legs, so their effect will partly cancel out when we take the difference $\Delta G_{ON} - \Delta G_{soln}$. This will significantly reduce any errors associated with the necessarily imperfect force field model, as shown previously.⁹ For example, although the $Mg^{2+}:P_i$ distances are systematically too short,⁹ the errors in the associated Coulomb interactions will cancel out when we subtract the protein and solution results.

To improve the convergence of the MD simulations, we apply harmonic restraints to the P_i in the protein binding pocket, which hold it in place while it is deleted.^{22–24} Therefore, the protein legs of each cycle include an initial step in which the restraint is introduced and a final step in which it is removed. For the sake of simplicity, these steps are not shown explicitly in Figure 1. The free energy ΔG_{rest}^{on} for introducing the restraint is computed numerically from the MD trajectory:²³ $\Delta G_{rest}^{on} = -kT \log \langle \exp(-U_{rest}/kT) \rangle$, where U_{rest} is the restraint energy and the brackets indicate an average over an MD simulation with the restraints absent. The free energy ΔG_{rest}^{off} to remove the restraint has a simple analytical form:

$$\Delta G_{rest}^{off} = kT \ln C(2\pi kT/k_h)^{3/2} \quad (1)$$

where k_h is the force constant for the harmonic restraint and C is the P_i concentration, which appears explicitly. Below, we use a force constant k_h of $2 \text{ kcal mol}^{-1} \text{ \AA}^{-2}$, so that for a 1 M standard state P_i concentration, $\Delta G_{\text{rest}}^{\text{off}} = -3.8 \text{ kcal/mol}$.

Molecular Dynamics Simulations. Structures of aIF2 from *S. solfataricus* in its ON, OFF, and MIXED conformations were taken from the Protein Data Bank (entries 2AHO, 2QN6, and 2QMU at crystallographic resolutions of 3.0, 2.5, and 3.2 Å, respectively).^{6,7} The γ and α domains are visible in the ON crystal structure, whereas the OFF structure includes a partial α domain. In the MIXED state, the complete β and γ domains are present, along with a partial α domain. Our MD simulations included protein residues within a sphere with a 26 Å radius, centered at the nucleotide center. Protein residues outside the sphere were eliminated; specifically, we retained residues that had at least one non-hydrogen atom within the sphere. A few crystal waters were included (2, 9, and 1 for the ON, OFF, and MIXED states, respectively). A cubic water box with a 74 Å edge was overlaid, and waters that overlapped with the protein, ligand, or crystal waters were removed. The final models included 12007, 12067, and 11606 waters (ON, OFF, and MIXED states, respectively). Protein atoms between 22 and 26 Å from the sphere's center ("buffer region") were harmonically restrained to their experimentally determined positions. Simulations were performed with periodic boundary conditions and the particle mesh Ewald method for long-range electrostatics (with "tin foil" boundary conditions).²⁸ The van der Waals interaction was spatially truncated at a 16 Å cutoff interatom distance. Five sodium ions were added to neutralize the overall charge of the ON and OFF MD models; one chloride ion was added to the MIXED state model. The temperature and pressure were maintained at 295 K and 1 bar, respectively. The temperature was controlled by using Langevin dynamics for the protein and solvent atoms other than hydrogens, with a coupling coefficient of 5 ps^{-1} . The pressure was controlled by a Langevin piston, Nose-Hoover method. The CHARMM22 force field was used for the protein and GTP/GDP^{25,26} and the TIP3P model for water.²⁹ Calculations were conducted with CHARMM³⁰ and NAMD.³¹

In both the ON and OFF crystal structures, the switch 1 loop is partly disordered, so that several amino acids are missing from the crystal structure:^{6,7} residues 36–43 in the ON state and residues 35–48 in the OFF state. The amino acids adjacent to these missing segments are within the 26 Å limit of our model, but rather distant from the ligand, especially its phosphate moieties; e.g., Ser35 is 10 Å from the β phosphate of GTP in the ON:GTP structure, while Met45 is 9 Å distant. On the basis of the overall orientation of the visible portion of switch 1, the missing amino acids are expected to be even more distant. Therefore, rather than attempting to model them explicitly, we have simply restrained the adjacent amino acids to stay close to their crystal positions, using harmonic restraints and a $4 \text{ kcal mol}^{-1} \text{ \AA}^{-2}$ force constant. Earlier work confirmed that this approximation had very little effect on the nucleotide specificities computed by MD.¹⁰ The complete switch 1 loop is present in the MIXED state; the backbone of the most distant residues, 41–46, is in the buffer region and is held in place by the weak, harmonic, buffer region restraints.

In the ON and OFF states, GDP was modeled in a fully deprotonated state, and P_i was modeled as HPO_4^{2-} , because they both coordinate a Mg^{2+} ion, which is known to strongly shift their pK_a values. In the MIXED state, there is no associated Mg^{2+} ion, so we performed additional simulations

specifically to determine the most plausible protonation state of GDP and P_i (reported in the Supporting Information), which identified GDP^{3-} and HPO_4^{2-} as the preferred states (as in the ON and OFF states). We also found that His97, a nearby amino acid, prefers to be doubly protonated in the MIXED state. In the ON and OFF states, it is farther from the P_i and is modeled as being singly protonated.

For the ON and OFF states, we created a model of the GDP and P_i complex as follows. We started from an MD simulation of the ON:GTP or OFF:GTP complex. We then cut the covalent bond between the β and γ phosphate, to produce GDP and P_i , and we allowed the P_i position to adjust through 100 steps of conjugate gradient energy minimization, with the protein and GDP fixed. We then equilibrated the new complex through 200 ps of MD with weak harmonic restraints applied to the protein backbone and, initially, its side chains.

MDFE Protocol for P_i Deletion. To convert P_i into a ghost particle, we use a hybrid energy function U that represents a mixture of the two end point states for the particular horizontal leg. U depends on two coupling coordinates, λ_{elec} and λ_{vdw} , which are used to scale the electrostatic and van der Waals energy terms, respectively:¹⁵

$$U = U(\lambda_{\text{elec}}, \lambda_{\text{vdw}}) = \lambda_{\text{elec}} U_{\text{elec}}^{P_i} + \lambda_{\text{vdw}} U_{\text{vdw}}^{P_i} \quad (2)$$

where $U_{\text{elec}}^{P_i}$ and $U_{\text{vdw}}^{P_i}$ represent the Coulombic and van der Waals interactions involving the P_i , respectively. By first varying λ_{elec} from 1 to 0 over a series of MD simulations, we remove the atomic charges of the HPO_4^{2-} . In a second series of simulations, we vary λ_{vdw} from 1 to 0, removing the P_i van der Waals interactions, leaving a ghost P_i in its place. From Boltzmann statistics, the free energy derivative with respect to either of the coupling constants can be written as $(\partial G)/(\partial \lambda) = \langle (\partial U)/(\partial \lambda) \rangle_\lambda$, where λ is λ_{elec} or λ_{vdw} and the brackets represent an average over an MD trajectory performed with a particular value of λ . For the alchemical transformation of the electrostatic term, the successive λ_{elec} values were 1.0, 0.9, 0.8, 0.7, 0.6, 0.5, 0.4, 0.3, 0.2, 0.1, and 0.0. Each simulation, or "window", lasted 0.6–2 ns. The last half of each window was used to estimate $\langle (\partial U)/(\partial \lambda) \rangle_\lambda$. For the van der Waals transformation, the successive λ_{vdw} values were 1.0, 0.9, 0.8, 0.7, 0.6, 0.5, 0.4, 0.3, 0.2, 0.1, 0.05, 0.01, and 0.001. Each simulation lasted 0.6–1.2 ns; the last half was used for averaging. The small, final λ_{vdw} values reflect a very gradual removal of the HPO_4^{2-} , to accurately account for the singularity of the free energy of particle removal.³² Although this procedure is probably less efficient than a protocol using a "soft-sphere" van der Waals potential for the vanishing P_i ,^{33,34} we expect that it is sufficiently accurate for our purposes (see the Supporting Information for more details). The energy derivatives were computed from a finite-difference estimate.⁹ We then calculated the free energy change using numerical integration.⁹ Trapezoidal integration was used for the electrostatic stage and for the van der Waals down to a λ_{vdw} of 0.05. Between 0.05 and 0, the van der Waals free energy derivative values were fit by a function of the form $A\lambda_{\text{vdw}}^B$,³² which was then integrated. The individual runs are detailed in the Supporting Information.

RESULTS

Dissociation of Phosphate from the ON and OFF States. The ON:GDP: P_i crystal structure is not known experimentally. The complex was modeled here by cutting

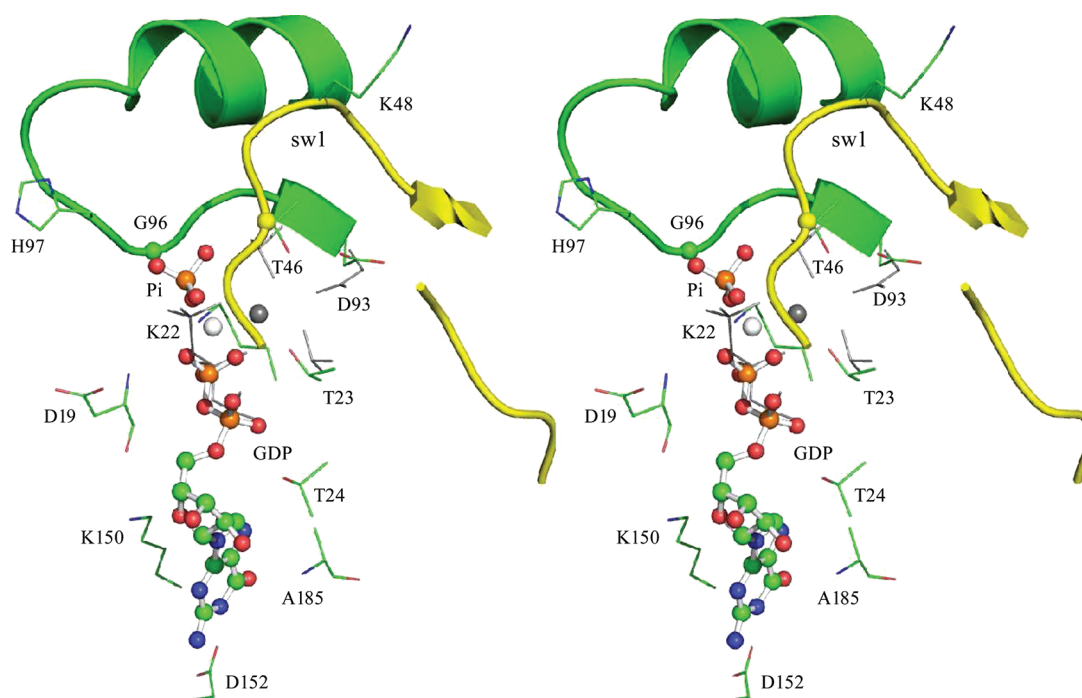


Figure 2. ON:GDP:Pi complex after 5 ns of molecular dynamics (cross-eyed stereoview). Switch 1 and switch 2 are colored yellow and green, respectively; GDP is shown as balls and sticks, and Mg^{2+} is shown as a white sphere. Selected groups from the starting, ON:GTP structure are shown for comparison, including the GTP phosphates (gray lines), the associated Mg^{2+} (gray sphere), Asp93, Thr23, and Thr46.

the bond between the β and γ phosphates in ON:GTP and allowing the product to gently relax (see Materials and Methods). The MD structure of the product is shown in Figure 2, superimposed on the initial, ON:GTP structure. The structure shown is also available as Supporting Information (along with similar structures for the OFF:GDP:Pi and MIXED:GDP:Pi complexes). Deviations between the two structures in Figure 2 are small: 0.6 Å for the protein main chain and 1.1 Å for side chains (averaging over non-hydrogen atoms within 22 Å of the center of the simulation sphere) and 0.7 Å for GDP. The P_i has moved by 1.7 Å (compared to the initial, γ phosphate position); the associated Mg^{2+} ion has moved by 1.8 Å, coming between the GDP and the P_i . A few side chains whose interaction with Mg^{2+} is broken have also shifted, especially Asp93 (Figure 2). The Mg^{2+} ion coordinates both the GDP β phosphate and P_i , each in a bidentate manner. Its coordination sphere is completed by two waters. Interatomic distances are listed in Table 1. The bridging Mg^{2+} promotes a rather short GDP– P_i distance of 4.4 ± 0.2 Å. The P_i also coordinates three to four waters, Thr46 from switch 1, Asp19, and Lys22 (Figure 2). The GDP α phosphate interacts with the Thr24 side chain and backbone.

The P_i dissociation free energy is computed using the thermodynamic cycle 1 in Figure 1. Deletion of P_i from the binding pocket gives a free energy of 419.7 kcal/mol. This value is an average over two 30 ns runs; details on the MD free energy convergence are given in the Supporting Information. There are also contributions from the harmonic spring used to restrain P_i as it is deleted (see Materials and Methods). The free energy for applying the restraint (before deletion), estimated from the MD simulations, is 0.2 kcal/mol. The free energy for removing it depends on the P_i concentration. With a standard state concentration of 1 M, we obtain a $\Delta G_{\text{rest}}^{\text{off}}$ of -3.8 kcal/mol. Overall, the free energy for deleting P_i in the protein (ΔG_{ON}) is thus

416.1 kcal/mol (Table 2). Deletion of P_i in solution, in the presence of a bound Mg^{2+} (as in the protein), gives a free energy ΔG_{soln} of 435.7 kcal/mol.⁹ There is an additional contribution from the initial, $\text{Mg}^{2+}:\text{P}_i$ binding step, which is known experimentally [$\Delta G_{\text{bind}}(\text{Mg}) = -3.7$ kcal/mol].²⁷ Overall, the standard binding free energy [$\Delta G_{\text{bind}}(\text{ON})$] is 15.9 kcal/mol (Table 2). Thus, dissociation of P_i from the ON state is extremely favorable. The resulting, ON:GDP complex can then relax spontaneously into the final, OFF:GDP product, because the free energy difference between them is ~ 2 kcal/mol, favoring OFF:GDP, as shown previously.¹⁰

Next, we consider dissociation of P_i from the OFF state. Results are similar to those for the ON state. The GDP– P_i distance is 4.5 ± 0.1 Å, and the GDP ligand deviates by just 0.8 Å from the initial, OFF:GTP structure (modeled previously¹⁰). Both P_i and the GDP β phosphate coordinate the Mg^{2+} in a bidentate manner, as before. The Mg^{2+} coordination sphere is completed by two waters. The P_i also interacts with Gly96 and with six to seven waters, compared to three to four in the ON state. Thus, the OFF binding pocket is significantly “wetter” than the ON pocket, as noted previously,¹⁰ and also the MIXED pocket (see below). Deleting P_i from the binding pocket gives a free energy ΔG_{OFF} of 412.1 kcal/mol, compared to 416.1 kcal/mol in the ON state. The ON versus OFF difference is thus 4.0 kcal/mol. The standard OFF:Pi binding free energy [$\Delta G_{\text{bind}}(\text{OFF})$] is 19.9 kcal/mol (Table 2). Therefore, dissociation of P_i from the OFF state is even more favorable than for the ON state.

A somewhat different aspect, also interesting, is to compare the ON:GDP:Pi free energy to that of the prehydrolysis, ON:GTP complex. For this, we decompose the ON:GTP \rightarrow ON:GDP:Pi hydrolysis reaction into four steps: ON:GTP unbinding, hydrolysis in solution, ON:GDP binding, and P_i binding. The hydrolysis free energy can then be

Table 1. Selected Interatomic Distances^a (angstroms) from MD Simulations

| interacting atoms | | MIXED X-ray | MIXED:GDP:P _i | ON:GDP:P _i | OFF:GDP:P _i |
|----------------------|-----------------------|-----------------|--------------------------|-----------------------|------------------------|
| Lys150 NZ | LIGA O4 | 3.97 | 3.33 (0.32) | 3.21 (0.30) | 3.29 (0.33) |
| Asp152 OD2 | LIGA H1 | 2.28 | 1.90 (0.14) | 2.68 (0.30) | 1.92 (0.16) |
| Asp152 OD1 | LIGA H22 | 2.76 | 1.79 (0.12) | 2.81 (0.30) | 1.81 (0.13) |
| Ala185 HN | LIGA O6 | 3.07 | 2.38 (0.21) | 2.29 (0.24) | 2.42 (0.23) |
| Thr24 HG1 | LIGA O1A | 1.83 | 1.77 (0.11) | 1.76 (0.12) | 1.80 (0.13) |
| Thr24 HN | LIGA O1A | 2.13 | 1.92 (0.12) | 1.91 (0.13) | 1.92 (0.12) |
| Thr23 HN | LIGA O3B | 4.50 | 1.92 (0.14) | 2.14 (0.24) | 2.30 (0.18) |
| Asp19 HN | LIGA O1B | 2.00 | 2.27 (0.24) | 2.52 (0.40) | 2.15 (0.23) |
| Lys22 HN | LIGA O2B | 2.29 | 1.93 (0.14) | 2.14 (0.22) | 1.96 (0.15) |
| Lys22 NZ | LIGA O2B | 3.94 | 2.62 (0.07) | 2.67 (0.09) | 2.70 (0.10) |
| His37 NE2 | LIGA O3B | 2.70 | 3.23 (0.22) | NA ^d | NA ^d |
| Mg | Thr23 OG1 | — | — | 3.69 (0.38) | 3.68 (0.25) |
| Mg | Thr46 OG1 | — | — | 4.36 (0.48) | NA ^d |
| Mg | LIGA O1B | — | — | 1.86 (0.06) | 1.86 (0.05) |
| Mg | LIGA O3B | — | — | 1.86 (0.06) | 1.89 (0.06) |
| Mg | Asp93 OD2 | — | — | 5.81 (0.91) | 6.49 (0.28) |
| Mg | P _i O3 | — | — | 2.47 (0.64) | 2.17 (0.52) |
| Mg | P _i O4 | — | — | 1.84 (0.08) | 1.89 (0.09) |
| Lys22 NZ | P _i O3 | 10.51 | 7.31 (0.25) | 2.64 (0.08) | 2.64 (0.08) |
| Lys22 NZ | P _i O4 | 8.68 | 5.31 (0.75) | 4.58 (0.27) | 4.70 (0.20) |
| His37 ND1 | P _i O3 | 3.79 | 2.74 (0.26) | NA ^d | NA ^d |
| His37 ND1 | P _i O4 | 2.73 | 3.75 (0.55) | NA ^d | NA ^d |
| His97 ND1 | P _i O1 | 4.07 | 3.41 (0.58) | 7.58 (0.79) | 8.34 (0.45) |
| His97 ND1 | P _i O2 | 5.25 | 2.80 (0.42) | 6.45 (0.36) | 7.80 (0.51) |
| Lys48 NZ | P _i O3 | 2.65 | 2.67 (0.09) | 15.84 (0.29) | NA ^d |
| Lys48 NZ | P _i O4 | 5.17 | 4.49 (0.37) | 14.76 (0.46) | NA ^d |
| Gly96 HN | P _i O4 | 5.63 | 2.30 (0.62) | 3.95 (0.22) | 4.99 (1.11) |
| P _i P1 | LIGA Pb | 7.03 | 6.46 (0.17) | 4.44 (0.10) | 4.50 (0.13) |
| Mg water | number ^b | — | — | 2.0 | 2.0 |
| Mg water | distance ^c | — | — | 2.00 (0.08) | 2.00 (0.07) |
| Pb water | number ^b | NA ^d | 2.0 | 1.2 | 1.1 |
| Pb water | distance ^c | NA ^d | 1.69 (0.10) | 1.84 (0.22) | 1.86 (0.20) |
| P _i water | number ^b | NA ^d | 4.09 | 3.51 | 6.5 |
| P _i water | distance ^c | NA ^d | 1.81 (0.21) | 1.88 (0.23) | 1.88 (0.22) |

^aStandard deviations in parentheses. ^bMean number of waters hydrogen bonding to the indicated group. ^cMean distance. ^dResidue or group absent from the X-ray structure or simulation model.

Table 2. HPO₄²⁻ Dissociation Free Energies (kilocalories per mole)

| state | deletion free energy | | dissociation free energy ^a |
|-------|----------------------|----------|---------------------------------------|
| | protein | solution | |
| MIXED | 400.5 | 399.7 | 0.8 |
| ON | 416.1 | 432.0 | −15.9 |
| OFF | 412.1 | 432.0 | −19.9 |

^aFree energy for dissociation of P_i from aIF2:GDP in each conformational state.

written:

$$\Delta G_{\text{hydr}}(\text{prot}) = \Delta G_{\text{hydr}}(\text{soln}) - \Delta \Delta G_{\text{ON}} + \Delta G_{\text{bind}}(\text{ON}) \quad (3)$$

where $\Delta G_{\text{hydr}}(\text{soln})$ is the free energy for GTP hydrolysis in solution (−7.3 kcal/mol), $\Delta G_{\text{bind}}(\text{ON})$ (15.9 kcal/mol) is the standard P_i + ON:GDP binding free energy (computed above), and $\Delta \Delta G_{\text{ON}} = \Delta G_{\text{bind}}(\text{ON,GTP}) - \Delta G_{\text{bind}}(\text{ON,GDP}) \approx -1$ kcal/mol is the free energy difference between GTP and GDP binding to the ON state, computed previously by MDfE.¹⁰ The two rightmost terms represent

the effect of the protein on the GTP hydrolysis free energy. We obtain a $\Delta G_{\text{hydr}}(\text{prot})$ of 9.6 kcal/mol and a $\Delta G_{\text{hydr}}(\text{prot}) - \Delta G_{\text{hydr}}(\text{soln})$ of 16.9 kcal/mol: the protein has an enormous, unfavorable effect on the hydrolysis free energy, as long as the P_i product remains in place in the binding pocket, 4.4 Å from the GDP β phosphate. Once P_i dissociates, the free energy drops by 15.9 kcal/mol [$\Delta G_{\text{bind}}(\text{ON})$]. The overall free energy, from ON:GTP to P_i + ON:GDP, is thus −6.3 kcal/mol, just 1 kcal/mol above the solution value. $\Delta G_{\text{hydr}}(\text{prot})$ is not known experimentally, but the time scale for GTP hydrolysis by the eukaryotic homologue eIF2 (in the absence of any GTPase-activating protein) is more than 28 h (the limit for experimental detection with the assay used).¹³ From transition state theory,³⁵ such a low rate is consistent with an activation free energy of more than 20 kcal/mol. Thus, while ON:GDP:P_i has a much higher free energy than ON:GTP, it is still well below the hydrolysis transition state.

Dissociation of Phosphate from the MIXED State. Figure 3 shows the structure of the MIXED state with bound GDP + P_i after 5 ns of MD. The structure is also available as Supporting Information. Selected groups from the structure after P_i dissociation are shown for comparison. The simulation structures agree well with the MIXED:GDP:P_i crystal structure;

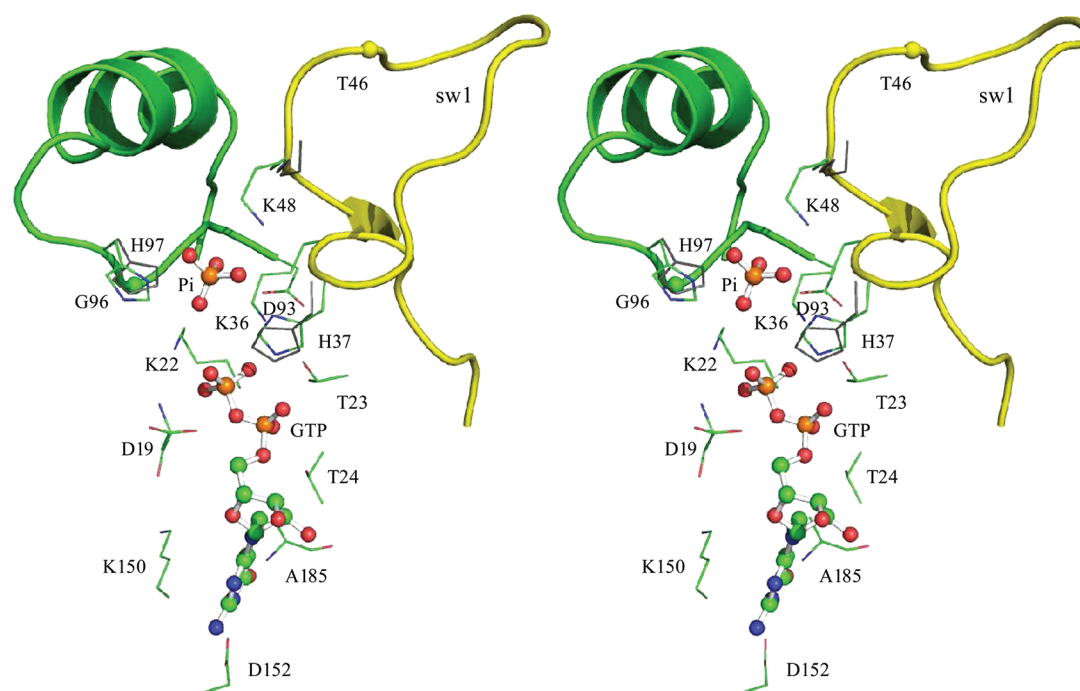


Figure 3. MIXED:GDP:Pi complex after 5 ns of molecular dynamics. Switch 1 and switch 2 are colored yellow and green, respectively. Three side chains from the postdissociation, MIXED:GDP structure are shown for comparison (gray lines): His37, His97, and Lys48. These side chains form a cluster of positive charge when P_i is present; Lys48 shifts away after P_i dissociates, unlike His37 and His97.

the root-mean-square deviation (rmsd) is 0.9 ± 0.1 Å for main chain atoms and 1.6 ± 0.1 Å for side chain atoms. The GDP ligand deviates by just 0.6 ± 0.1 Å; the average GDP- P_i distance is 6.5 ± 0.2 Å, compared to 7.0 Å in the crystal structure. The rmsds for switch 1 (residues 31–51) and switch 2 (residues 93–113) are 1.5 ± 0.1 and 1.0 ± 0.1 Å, respectively. Unlike the ON and OFF states, above, the nucleotide has no bound Mg^{2+} ion (Figure 3). The Mg^{2+} position is taken by His37, from switch 1, whose side chain forms a salt bridge with both P_i and the GDP β phosphate (Table 1). Switch 1 has a peculiar conformation, neither ON nor OFF; switch 2 is in the ON conformation. Because of its position, His37 is assumed to be doubly protonated and positively charged. The ligands are modeled as GDP^{3-} and HPO_4^{2-} , based on pK_a calculations, reported in the Supporting Information. Another histidine side chain, His97, also interacts directly with P_i and is predicted to be positively charged. The Lys48 side chain, from switch 1, also interacts directly with P_i . The phosphate accepts hydrogen bonds from four waters on average, compared to 14 in solution.⁹ Thus, the availability of water in the MIXED binding pocket is significantly reduced. The GDP α phosphate accepts hydrogen bonds from the Thr24 side chain and backbone; its β phosphate accepts hydrogen bonds from the Asp19 and Lys22 backbones and two waters and makes a salt bridge with the Lys22 side chain. When P_i dissociates, it leaves behind an electrostatic “hole”, so that the cluster of positive side chains formed by His37, His97, and Lys48 rearranges, with Lys48 shifting away (Figure 3). Another possibility would be for His97 to lose a proton and become neutral after P_i dissociation. In fact, we show (Supporting Information) that the P_i binding free energy is insensitive to the His97 protonation state. This indicates that the P_i group does not shift the His97 pK_a , so the protonation state does not change when P_i dissociates.

To compute the P_i binding free energy, we use the thermodynamic cycle 2 in Figure 1. The free energy for deleting P_i from the binding pocket is estimated to be 404.0 kcal/mol (Table 2). Another -3.5 kcal/mol comes from the harmonic restraints that hold the P_i in place while it is deleted. Overall, the free energy for the protein leg (ΔG_{MIXED}) is 400.5 kcal/mol. The free energy for deletion in solution, $\Delta G'_{\text{soln}}$, was computed earlier to be 399.7 kcal/mol.⁹ Taking the difference, we obtain the standard binding free energy $\Delta G_{\text{bind}}(\text{MIXED}) = -0.8$ kcal/mol. If His97 is modeled in a singly protonated form, results are very similar (Supporting Information).

Overall, binding of P_i to the MIXED state is weakly favorable. The favorable binding can be understood in terms of the ionic interactions between P_i and His37, Lys48, and His97, and four waters, which offset the P_i -GDP repulsion as well as the strong interactions between HPO_4^{2-} and bulk solvent in the unbound state. Notice that the binding reactions considered here and above start from a protein already preorganized in a particular conformational state, MIXED in this case. In solution, aIF2:GDP exists as a mixture of the ON, OFF, and MIXED states, with OFF:GDP being the predominant state. For binding of P_i to such a mixture, there is an additional free energy contribution, which corresponds approximately to the OFF:GDP \rightarrow MIXED:GDP free energy difference.¹⁰ This last free energy is positive but unknown; it could be deduced from an experimental measurement of the aIF2: P_i binding constant (not available so far).

Comparing the ON, OFF, and MIXED States. So far, we have considered the aIF2 states individually and compared the stability of each one with and without bound P_i . In particular, we have shown that the ON:GDP: P_i posthydrolysis complex is very unstable, since its free energy can be lowered considerably by phosphate dissociation. A second possibility is for ON:GDP: P_i to relax into the OFF state. We show below that the corresponding free energy is most likely positive (opposing

relaxation) but not very large. If the system does reach the OFF:GDP:P_i state, P_i dissociation is again extremely favorable. A third possibility is for ON:GDP:P_i to relax into the MIXED state, consistent with the idea that the MIXED state is a stable intermediate, populated after GTP hydrolysis and before phosphate release.^{7,13} To test this, we should compare the stabilities of ON:GDP:P_i and MIXED:GDP:P_i. Unfortunately, converting ON:GDP:P_i into MIXED:GDP:P_i involves a large conformational change, whose free energy is hard to obtain from simulations. Here, we obtain a much more limited result: we show that the ON:GDP:P_i → MIXED:GDP:P_i free energy is much smaller than the ON:GDP → MIXED:GDP free energy. Therefore, the MIXED:GDP:P_i free energy can only be higher than that of ON:GDP:P_i if the MIXED:GDP versus ON:GDP free energy difference is very large.

To compare ON:GDP:P_i and OFF:GDP:P_i, we use the thermodynamic cycle shown in Figure 4. The horizontal legs

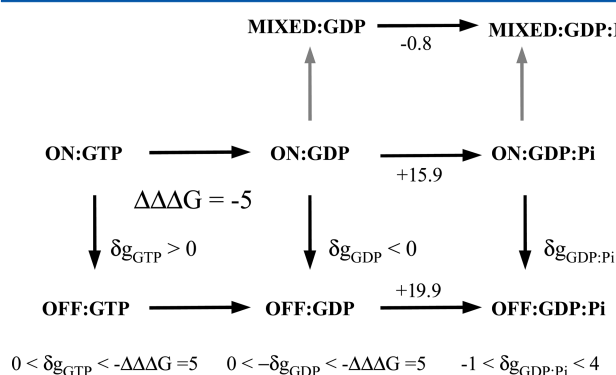


Figure 4. Thermodynamic cycle for comparing ON:GDP:P_i, ON:GDP, and MIXED:GDP:P_i. Free energies (kilocalories per mole) for some of the legs are indicated.

correspond to the binding or unbinding of a ligand: GTP, GDP, or P_i. Previously, we compared the GTP and GDP binding free energies in both the ON and OFF states. With the notations defined earlier, we obtained a $\Delta\Delta G_{\text{ON}}$ of -1 ± 2 kcal/mol (favoring GTP) and a $\Delta\Delta G_{\text{OFF}}$ of 4 ± 2 kcal/mol (favoring GDP),¹⁰ giving $\Delta\Delta\Delta G = \Delta\Delta G_{\text{ON}} - \Delta\Delta G_{\text{OFF}} = -5 \pm 2.8$ kcal/mol.

To compare the ON versus OFF stabilities with a given ligand, we should simulate the vertical legs in Figure 4, which is more challenging. Experimental data provide some inequalities. Thus, the OFF:GDP free energy is presumably lower than the ON:GDP free energy, whereas the ON:GTP free energy is lower than the OFF:GTP free energy. We then have

$$\begin{aligned} \Delta G(\text{OFF:GDP} \rightarrow \text{ON:GDP}) \\ = \Delta G(\text{OFF:GTP} \rightarrow \text{ON:GTP}) - \Delta\Delta\Delta G \end{aligned} \quad (4)$$

$$\begin{aligned} 0 < \Delta G(\text{OFF:GDP} \rightarrow \text{ON:GDP}) < -\Delta\Delta\Delta G \\ = 5 \text{ kcal/mol} \end{aligned} \quad (5)$$

Furthermore, we have

$$\begin{aligned} \Delta G(\text{ON:GDP:P}_i \rightarrow \text{OFF:GDP:P}_i) \\ = \Delta G(\text{ON:GDP} \rightarrow \text{OFF:GDP}) \\ + \Delta G_{\text{bind}}(\text{OFF}) - \Delta G_{\text{bind}}(\text{ON}) \end{aligned} \quad (6)$$

The difference between P_i binding free energies on the right is 4.0 kcal/mol, so that

$$\begin{aligned} -1.0 \text{ kcal/mol} < \Delta G(\text{ON:GDP:P}_i \rightarrow \text{OFF:GDP:P}_i) \\ < 4.0 \text{ kcal/mol} \end{aligned} \quad (7)$$

A negative value for the ON:GDP:P_i → OFF:GDP:P_i reaction is thus possible, but only if the ON:GTP versus OFF:GTP stability difference is less than 1.0 kcal/mol. If we assume it is at least 0.5 kcal/mol and take into account the statistical uncertainty of $\Delta\Delta\Delta G$, our best estimate for the ON:GDP:P_i → OFF:GDP:P_i free energy is 2 ± 3.5 kcal/mol. We may conclude that the ON:GDP:P_i → OFF:GDP:P_i free energy can be weakly negative but is more likely to be positive, opposing spontaneous relaxation.

Finally, we consider the relative free energies of the MIXED and ON complexes with either GDP or GDP + P_i. As in eq 6, we have

$$\begin{aligned} \Delta G(\text{ON:GDP:P}_i \rightarrow \text{MIXED:GDP:P}_i) \\ = \Delta G(\text{ON:GDP} \rightarrow \text{MIXED:GDP}) \\ + \Delta G_{\text{bind}}(\text{MIXED}) - \Delta G_{\text{bind}}(\text{ON}) \end{aligned} \quad (8)$$

The difference between the P_i binding free energies on the right is large and negative [-16.7 kcal/mol (Table 2)]. Therefore, the MIXED:GDP:P_i complex is much lower in free energy, relative to ON:GDP:P_i, than the MIXED:GDP complex, relative to ON:GDP. Because OFF:GDP is below ON:GDP, we may conclude that MIXED is the most stable state for aIF2:GDP:P_i if, and only if, the ON:GDP → MIXED:GDP free energy is less than 16.7 kcal/mol. In that case, spontaneous relaxation from the posthydrolysis ON:GDP:P_i complex would be thermodynamically possible.

DISCUSSION

To carry out its function, aIF2 exists as a mixture of conformational states, ON, OFF, and possibly MIXED, whose populations are modulated by the nucleotide ligands. Thus, apo-aIF2 and aIF2:GDP are predominantly OFF; aIF2:GTP can be ON or OFF, and aIF2:GDP:P_i can be MIXED and possibly ON. To understand the mechanism in depth, we should determine the relative stabilities of all the intermediates along several possible aIF2 reaction paths, discussed above and schematized in Figure 5. Our MD simulations provide some of

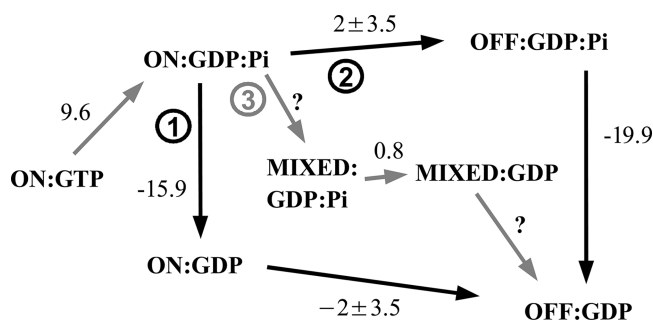


Figure 5. Three pathways connecting the posthydrolysis ON:GDP:P_i complex to the final OFF:GDP product. Free energies computed here are given (in kilocalories per mole).

this information. Earlier, we computed the GTP/GDP binding free energy differences in the ON and OFF states.¹⁰ Their difference, $\Delta\Delta\Delta G$, was shown to be -5.0 ± 2.8 kcal/mol,

arising from a small ON state specificity and a rather large OFF state specificity. Here, we computed the free energies for binding of inorganic phosphate to aIF2 in each individual state: ON, OFF, and MIXED. We found that the MIXED state has a weak binding affinity, while the other states have essentially no binding affinity. In particular, dissociation of phosphate from ON:GDP:P_i is highly favorable.

Our main goal was to compare three possible posthydrolysis steps and to test, at least partly, the idea that the MIXED state seen in a crystal structure is a stable intermediate, populated after GTP hydrolysis and before phosphate release. We showed that the posthydrolysis complex, ON:GDP:P_i, is very unstable with respect to phosphate dissociation (pathway 1 in Figure 5). We also showed that transformation into OFF:GDP:P_i (pathway 2) can be weakly downhill but is more likely a weakly uphill process. Going all the way from the ON:GTP reactant state to the OFF:GDP product, regardless of the pathway, our best estimate of the total free energy change is -8.3 ± 3.5 kcal/mol. Unfortunately, we could not compute the free energy for transformation into MIXED:GDP:P_i (pathway 3), to test whether it could be a stable intermediate. We were able to show, however, that for MIXED:GDP:P_i to be higher in free energy than the posthydrolysis state, the MIXED:GDP complex would have to be very unstable indeed. Overall, our data cannot fully determine which step, 1, 2, or 3, is the most favored thermodynamically (let alone kinetically), but it does provide a rather detailed qualitative picture of the aIF2 free energy landscape.

If P_i dissociates first, the next state is ON:GDP, which, in turn, has a rather high (predicted) free energy compared to that of the final product, OFF:GDP.¹⁰ On the other hand, if conformational relaxation into the MIXED state occurs first, another question arises: does Mg²⁺ dissociate, to give the Mg²⁺-free complex seen in the crystal structure and simulated in this work? Does it dissociate before or after the ON → MIXED conformational relaxation? It is very difficult to answer this last question computationally, because it would require the calculation of aIF2:GDP:Mg²⁺ dissociation free energies, which is hard to do accurately using current force fields.⁹ For the moment, we have simply assumed, on the basis of the crystal structure, that the relevant MIXED complex is Mg²⁺-free.

This study illustrates some of the difficulties involved in obtaining a complete description of the mechanism of aIF2, even in vitro, with its multiple functional conformations and nucleotide ligands. Computer simulations, despite their limitations, are valuable for characterizing the main states and their thermodynamic properties individually. In the future, they also have the potential to characterize the free energy contributions of the other, major biological partners: initiator tRNA, the ribosome, and other initiation factors.

■ ASSOCIATED CONTENT

● Supporting Information

A description of the free energy calculations for determining the protonation of GDP, P_i, and a protein side chain in the MIXED state, details of the uncertainty of the MD free energy simulations, and one structure from each of three MD simulations, corresponding to the three protein states (ON, OFF, and MIXED) with bound GDP + P_i (PDB format). This material is available free of charge via the Internet at <http://pubs.acs.org>.

■ AUTHOR INFORMATION

Corresponding Author

*E-mail: thomas.simonson@polytechnique.fr. Phone: 33-169334860. Fax: 33-169334909.

■ ACKNOWLEDGMENTS

We thank Yves Mechulam and Emmanuelle Schmitt for helpful discussions. Some of the calculations were conducted at the CINES supercomputer center of the French Ministry of Research.

■ ABBREVIATIONS

aIF2, archaeal initiation factor 2; MDFF, molecular dynamics free energy.

■ REFERENCES

- (1) Sprang, S. R. (1997) G proteins, effectors and GAP's: Structure and mechanism. *Curr. Opin. Struct. Biol.* 7, 849–856.
- (2) Vetter, I. R., and Wittinghofer, A. (2001) The guanine nucleotide-binding switch in three dimensions. *Science* 294, 1299–1304.
- (3) Hauryliuk, V. V. (2006) GTPases of the prokaryotic translation apparatus. *Mol. Biol.* 40, 688–701.
- (4) Myasnikov, A. G., Simonetti, A., Marzi, S., and Klaholz, B. P. (2009) Structure-function insights into prokaryotic and eukaryotic translation initiation. *Curr. Opin. Struct. Biol.* 19, 300–309.
- (5) Grant, B. J., Gorfe, A. A., and McCammon, J. A. (2010) Large conformational changes in proteins: Signalling and other functions. *Curr. Opin. Struct. Biol.* 20, 142–147.
- (6) Yatime, L., Mechulam, Y., Blanquet, S., and Schmitt, E. (2006) Structural switch of the γ subunit in an archaeal aIF2 $\alpha\gamma$ heterodimer. *Structure* 14, 119–128.
- (7) Yatime, L., Méchulam, Y., Blanquet, S., and Schmitt, E. (2007) Structure of an archaeal heterotrimeric initiation factor 2 reveals a nucleotide state between the GTP and the GDP states. *Proc. Natl. Acad. Sci. U.S.A.* 104, 18445–18450.
- (8) Nikonov, O., Stolboushina, E., Nikulin, A., Hasenohrl, D., Blasi, U., Manstein, D., Fedorov, R., Garber, M., and Nikonov, S. (2007) New insights into the interactions of the translation initiation factor 2 from archaea with guanine nucleotides and initiator tRNA. *J. Mol. Biol.* 373, 328–336.
- (9) Satpati, P., Clavaguéra, C., Ohanessian, G., and Simonson, T. (2011) Free energy simulations of a GTPase: GTP and GDP binding to archaeal initiation factor 2. *J. Phys. Chem. B* 115, 6749–6763.
- (10) Satpati, P., and Simonson, T. (2012) Conformational selection through electrostatics: Free energy simulations of GTP and GDP binding to archaeal Initiation Factor 2. *Proteins*, in press.
- (11) Koetting, C., Bleszenohl, M., Suveyzdis, Y., Goody, R. S., Wittinghofer, A., and Gerwert, K. (2006) A phosphoryl transfer intermediate in the GTPase reaction of Ras in complex with its GTPase-activating protein. *Proc. Natl. Acad. Sci. U.S.A.* 103, 13911–13916.
- (12) Kothe, U., and Rodnina, M. V. (2006) Delayed release of inorganic phosphate from elongation factor Tu following GTP hydrolysis on the ribosome. *Biochemistry* 45, 12767–12774.
- (13) Algire, M. A., Maag, D., and Lorsch, J. R. (2005) Pi release from eIF2, not GTP hydrolysis, is the step controlled by start-site selection during eukaryotic translation initiation. *Mol. Cell* 20, 251–262.
- (14) Kollman, P. (1993) Free energy calculations: Applications to chemical and biochemical phenomena. *Chem. Rev.* 93, 2395.
- (15) Simonson, T., Archontis, G., and Karplus, M. (2002) Free energy simulations come of age: The protein–ligand recognition problem. *Acc. Chem. Res.* 35, 430–437.
- (16) Jorgensen, W. L. (2003) The many roles of computation in drug discovery. *Science* 303, 1813–1818.
- (17) Thompson, D., and Simonson, T. (2006) Molecular dynamics simulations show that bound Mg²⁺ contributes to amino acid and

aminoacyl adenylate binding specificity in aspartyl-tRNA synthetase through long range electrostatic interactions. *J. Biol. Chem.* 281, 23792–23803.

(18) Pfaendtner, J., Branduardi, D., Parrinello, M., Pollard, T. D., and Voth, G. A. (2007) Nucleotide-dependent conformational states of actin. *Proc. Natl. Acad. Sci. U.S.A.* 106, 12723–12728.

(19) Yang, W., Gao, Y. Q., Cui, Q., Ma, J., and Karplus, M. (2003) The missing link between thermodynamics and structure in F1-ATPase. *Proc. Natl. Acad. Sci. U.S.A.* 100, 874–879.

(20) Gao, Y. Q., Yang, W., and Karplus, M. (2005) A structure-based model for the synthesis and hydrolysis of ATP by F1-ATPase. *Cell* 123, 195–205.

(21) Khavrutskii, I. V., Grant, B., Taylor, S. S., and McCammon, J. A. (2009) A transition path ensemble study reveals a linchpin role for Mg^{2+} during rate-limiting ADP release from protein kinase A. *Biochemistry* 48, 11532–11545.

(22) Jorgensen, W., Buckner, K., Boudon, S., and Tirado-Rives, J. (1988) Efficient computation of absolute free energies of binding by computer simulations. Application to the methane dimer in water. *J. Chem. Phys.* 89, 3742–3746.

(23) Simonson, T. (2001) in *Computational Biochemistry & Biophysics* (Becker, O., Mackerell, A., Jr., Roux, B., and Watanabe, M., Eds.) Marcel Dekker, New York.

(24) Deng, Y., and Roux, B. (2009) Computations of standard binding free energies with molecular dynamics simulations. *J. Phys. Chem. B* 113, 2234–2246.

(25) Mackerell, A. D., Wiorkiewicz-Kuczera, J., and Karplus, M. (1995) An all-atom empirical energy force-field for the study of nucleic acids. *J. Am. Chem. Soc.* 117, 11946–11975.

(26) Mackerell, A. D., Bashford, D., Bellott, M., Dunbrack, R. L., Evanseck, J., Field, M. J., Fischer, S., Gao, J., Guo, H., Ha, S., Joseph, D., Kuchnir, L., Kuczera, K., Lau, F. T. K., Mattos, C., Michnick, S., Ngo, T., Nguyen, D. T., Prodhom, B., Reiher, W. E., Roux, B., Smith, J., Stote, R., Straub, J., Watanabe, M., Wiorkiewicz-Kuczera, J., Yin, D., and Karplus, M. (1998) An all-atom empirical potential for molecular modelling and dynamics study of proteins. *J. Phys. Chem. B* 102, 3586–3616.

(27) Alberty, R. A., and Goldberg, R. N. (1992) Standard thermodynamic formation properties for the adenosine 5'-triphosphate series. *Biochemistry* 31, 10610–10615.

(28) Darden, T., York, D., and Pedersen, L. (1993) Particle mesh Ewald: An $N \log(N)$ method for Ewald sums in large systems. *J. Chem. Phys.* 98, 10089–10092.

(29) Jorgensen, W., Chandrasekar, J., Madura, J., Impey, R., and Klein, M. (1983) Comparison of simple potential functions for simulating liquid water. *J. Chem. Phys.* 79, 926–935.

(30) Brooks, B., Brooks, C. L. III, Mackerell, A. D. Jr., Nilsson, L., Petrella, R. J., Roux, B., Won, Y., Archontis, G., Bartels, C., Boresch, S., Caffisch, A., Caves, L., Cui, Q., Dinner, A. R., Feig, M., Fischer, S., Gao, J., Hodoscek, M., Im, W., Kuczera, K., Lazaridis, T., Ma, J., Ovchinnikov, V., Paci, E., Pastor, R. W., Post, C. B., Pu, J. Z., Schaefer, M., Tidor, B., Venable, R. M., Woodcock, H. L., Wu, X., Yang, W., York, D. M., and Karplus, M. (2009) CHARMM: The biomolecular simulation program. *J. Comput. Chem.* 30, 1545–1614.

(31) Phillips, J. C., Braun, R., Wang, W., Gumbart, J., Tajkhorshid, E., Villa, E., Chipot, C., Skeel, R. D., Kale, L., and Schulten, K. (2005) Scalable molecular dynamics with NAMD. *J. Comput. Chem.* 26, 1781–1802.

(32) Simonson, T. (1993) Free energy of particle insertion. An exact analysis of the origin singularity for simple liquids. *Mol. Phys.* 80, 441–447.

(33) Steinbrecher, T., Mobley, D. L., and Case, D. A. (2007) Nonlinear scaling schemes for Lennard-Jones interactions in free energy calculations. *J. Chem. Phys.* 127, 214108.

(34) Bruckner, S., and Boresch, S. (2011) Efficiency of alchemical free energy simulations II: Improvements for thermodynamic integration. *J. Comput. Chem.* 32, 1320–1333.

(35) Straub, J. (2001) in *Computational Biochemistry & Biophysics* (Becker, O., Mackerell, A., Jr., Roux, B., and Watanabe, M., Eds.) Marcel Dekker, New York.